

# Daytime ionospheric absorption features in the polar cap associated with poleward drifting *F*-region plasma patches

Masanori Nishino<sup>1</sup>, Satonori Nozawa<sup>1</sup>, and Jan A. Holtet<sup>2</sup>

<sup>1</sup>*Solar-Terrestrial Environment Laboratory, Nagoya University, Toyokawa, Japan*

<sup>2</sup>*Department of Physics, University of Oslo, Oslo, Norway*

(Received April 9, 1997; Revised December 6, 1997; Accepted December 26, 1997)

Absorption of radio waves in the polar ionosphere near the magnetic noon was observed on October 8, 1991, by the 30 MHz imaging riometer at Ny-Alesund, Svalbard (invariant latitude 76.1°). These observations showed that the initially widespread absorption features became localized and enhanced in the high-latitude sector of the field of view, and followed a poleward motion. This behavior occurred quasi-periodically and repeated every 10–20 min. Simultaneous observations by EISCAT “Polar” experiments showed that nine discrete plasma patches, with *F*-region electron density enhanced by an order of  $10^6$  el/cm<sup>3</sup>, drifted poleward from the polar cusp to the cap during the same period. This coincidence suggested that the ionospheric absorption was associated with *F*-region plasma patches in the polar cap. Theoretical absorption values of 0.14 dB, estimated using the electron densities and the electron-ion collision frequencies from the EISCAT *F*-region plasma data, are smaller than the observed values (<0.8 dB). This discrepancy may be related to the difference between the theoretically- and experimentally-determined collision frequencies, as indicated by Wang *et al.* (1994). These localized, enhanced, and poleward drifting absorption features over Ny-Alesund may be explained as *F*-region plasma patches produced by a magnetosheath-like particle precipitation into the cusp, and as small-scale irregularities caused by density gradients of the patches drifting into the polar cap.

## 1. Introduction

The absorption of cosmic radio waves in the ionosphere is usually measured by a riometer (Relative Ionospheric Opacity meter) in the frequency range of 20–50 MHz. Ionospheric absorption in the polar region occurs mainly in the *D* or lower *E*-region, where electrons, with density enhanced by the precipitation of energetic-electrons with energy from several to several tens of keV, collide with the neutral particles. Recent developments in imaging riometer for ionospheric study (IRIS) techniques (e.g., Detrick and Rosenberg, 1990) have enabled new and interesting observations of the complex dynamics of the ionospheric absorption features in the auroral and polar-cap regions to be carried out. Amongst the various types of riometer absorption reviewed by Stauning (1996a), daytime absorption features observed by the Sondre Stromfjord (73.5° invariant latitude) imaging riometer were attributed to an increased *E*-region collision frequency associated with strong electric fields in the polar ionosphere (Stauning, 1984; Stauning and Olesen, 1989). Using data taken by the imaging riometer at Sondre Stromfjord, Stauning (1996b) presented IMF (interplanetary magnetic field)-dependent poleward progressing absorption features in the *E*-region ionosphere. This type of disturbance has been considered to be the “footprints” in the ionosphere of the *B<sub>y</sub>*-component of the IMF (in an open magnetospheric configuration), which convected across the polar cap. Using the three imaging riometers at cusp-latitude, Nishino *et al.* (1997)

showed that this type of absorption feature had an anti-sunward motion, with a front-like feature extending over 700 km in longitude.

Using measurements near the magnetic noon by the 38.2 MHz imaging riometer at the South Pole (−74.2° invariant latitude), Rosenberg *et al.* (1993) recently revealed another class of unusual daytime absorption phenomenon in a dark ionosphere. These could reach values in excess of 1 dB. Since there was no corresponding change in the N<sub>2</sub><sup>+</sup> 427.8-nm auroral emission, Rosenberg *et al.* suggested that this type of absorption was unlikely to be caused by the increase in ionization in the *D* or lower *E* region, usually attributed to the precipitation of auroral electrons of keV energy. Rather, the absorption features were shown to be related to the *F*-region electron density structures drifting from the dayside cusp into the polar cap, by comparison with the ionosonde data at the South Pole, and with the HF radar data collected by the Polar Anglo-American Conjugate Experiment (PACE) at Halley, Antarctica. It seems, however, that the absorption features in the *F*-region remain somewhat controversial. Wang *et al.* (1994) observed a pre-noon absorption event of 0.3 dB relating to drifting *F*-region plasma patches passing at an altitude of 300–400 km, in a sunlit ionosphere overhead Sondre Stromfjord. They derived absorption values of 0.07 dB, using the *F*-region electron densities and temperatures obtained from simultaneous observations by incoherent scatter (IS) radar. By comparison with the ionosonde measurements, Wang *et al.* indicated that the pre-noon absorption might be caused by the enhanced electron density of *F*-region plasma patches drifting into the polar cap. The dynamic behavior of the absorption structures in the spatial

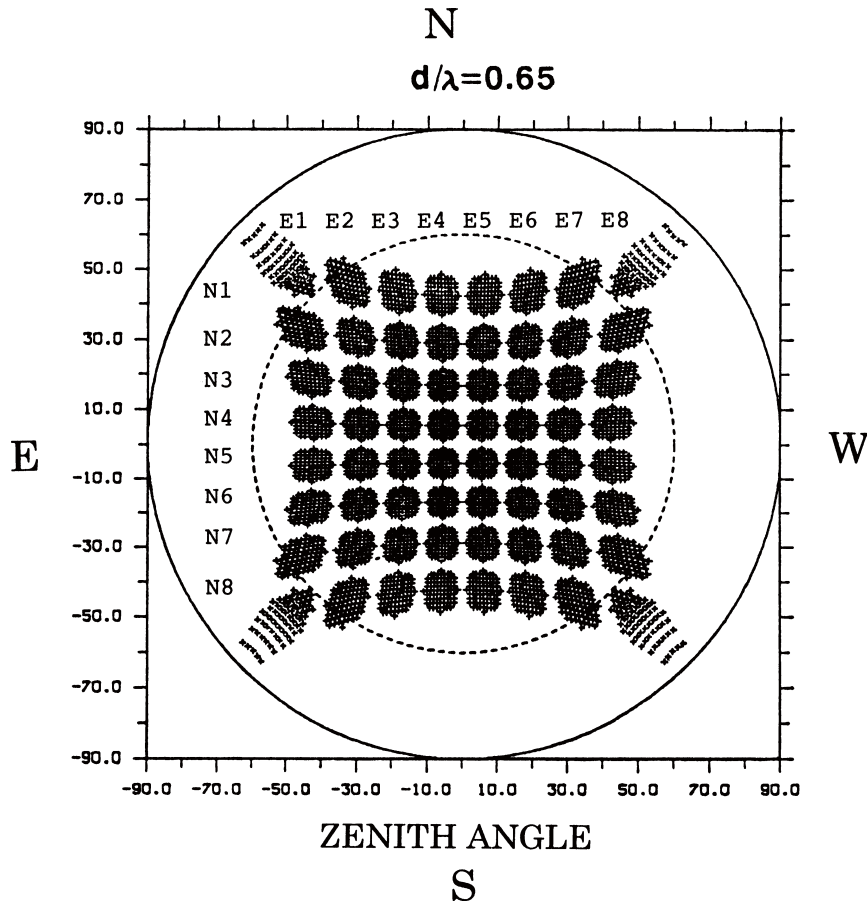


Fig. 1. The two-dimensional  $8 \times 8$  beams of the imaging riometer (IRIS) installed at Ny-Alesund, Svalbard, with zenith angle indicated. Also drawn are the half-power areas of individual beams, where the dipole spacing is 0.65 times the wavelength (adapted from Yamagishi *et al.*, 1992). The beams are assigned to labels N1, N2, ..., N8 from the geomagnetic north to south, and E1, E2, ..., E8 from the geomagnetic east to west.

and temporal scale, however, was not demonstrated.

In this paper we report the observation by the imaging riometer (IRIS) at Ny-Alesund, Svalbard ( $76.1^\circ$  invariant latitude) of an ionospheric absorption event near the magnetic noon on October 8, 1991. The observed daytime absorption event, which appeared quasi-periodically, is characterized by the poleward motion of a localized enhancement in the IRIS field. The maximum absorption values of about 0.8 dB reached are compared with the values calculated using the ionospheric plasma data observed simultaneously by the EISCAT IS radar at Tromsø in Norway. Also discussed is the dynamic behavior of the daytime absorption structures, by relating them with the  $F$ -region plasma patches drifting from the cusp into the polar cap.

## 2. Ionospheric Absorption Data

The IRIS antenna at Ny-Alesund consists of a two-dimensional  $8 \times 8$  element dipole-array with a half-wavelength at 30 MHz, which is approximately aligned with the geomagnetic north-south and east-west directions. The antenna produces a two-dimensional array of  $8 \times 8$  beams, directed upward within zenith angles of  $\pm 45^\circ$ , as shown in Fig. 1, where the dipole spacing is taken as 0.65 times the wavelength. The half-power width of an individual beam is  $11^\circ$ . The beams in the field of view are labeled N1, N2, ..., N8 from the geomagnetic north to south, and E1, E2, ..., E8 from

the geomagnetic east to west. The IRIS technique and data handling procedures are described in detail by Nishino *et al.* (1993) and Yamagishi *et al.* (1992).

Stack plots of time-varying absorption intensities, observed at Ny-Alesund during 0700–1100 UT on October 8, 1991, are shown in Fig. 2. They correspond to the eight-beams in the east-west cross-section which pass through the third most northern row (N3), and those in the north-south cross-section which pass through the second most western column (E7). They represent the time-averaged values over 16 sec in a 1.0 dB/div scale. Since the local magnetic noon at Ny-Alesund is at approximately 0830 UT, the detection of absorption is definitely a daytime event near the magnetic noon. From this figure, it is predicted that the absorption features show a northward (poleward) motion during 0730–0740 UT, and the subsequent absorption features show northward motions with eastward components during 0745–1020 UT.

Plate 1 displays a time-series of ionospheric absorption images produced from the 64 IRIS-beams, taken during the period 0708:56–0907:55 UT. Each image is an average over one minute. Absorption values up to 1.0 dB are represented in the color-bar. The plot is orientated with the geomagnetic north pointing upwards and the geomagnetic west pointing to the right. The IRIS field of view covers an area of  $600 \text{ km} \times 600 \text{ km}$ , assuming an ionospheric height of 300 km.

OCTOBER 8 1991 NY-ALESUND

Scale: 1.0 dB/div

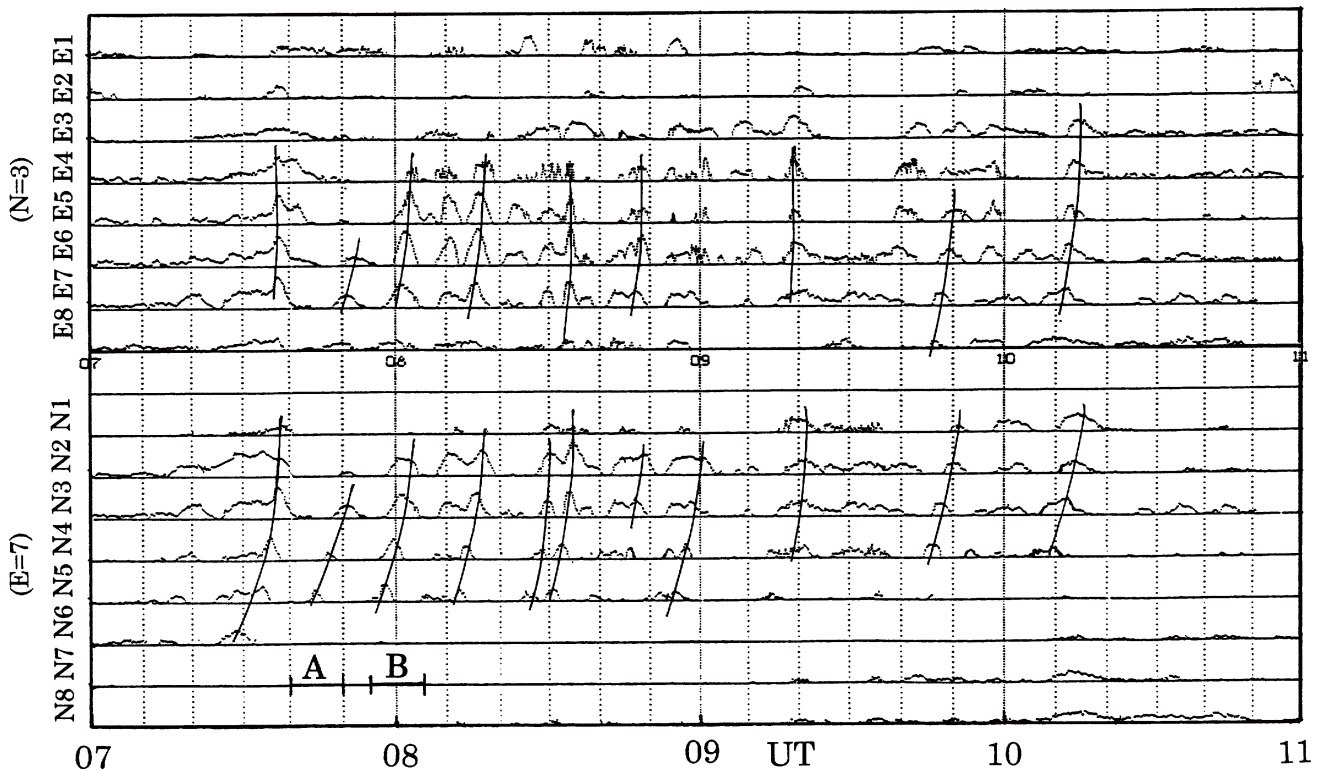


Fig. 2. The time-varying absorption intensities for the eight-beams in the east-west cross-section passing through the third-northernmost row (N3), and those in the north-south cross-section passing through the second-westernmost column (E7), observed at Ny-Alesund during 0700–1100 UT on October 8, 1991.

Around 0730 UT, the absorption spreads in the central area of the IRIS field, and shows some patchy structures with weak intensities less than 0.6 dB. At about 0740 UT, the structures are extended in a sheet-like shape orientated in the east-west direction in the high-latitude sector of the IRIS field. With a 0.8 dB enhancement, the feature has a small spatial scale, and follows a northward (poleward) motion. The speed of the moving absorption feature is estimated to be about 1.0 km/s, assuming an ionospheric absorption height of 300 km. Similar features appear quasi-periodically at about 0800 UT, 0815 UT, 0835 UT, 0845 UT and 0858 UT, yielding a repetition period of 10–20 min. These structures are more localized to a small area scale (~300 km), particularly at 0800 UT and 0815 UT, and show poleward motions (0.5–1.0 km/s) with eastward components. These speeds are nearly equivalent to those of the absorption features at a height of 300 km estimated by Rosenberg *et al.* (1993). Note that prominent spots in the north-east sector between about 0834 and 0843 UT represent false absorption, caused by the ionospheric scintillation effects of the radio stars in Cassiopeia.

### 3. EISCAT Data

Lockwood and Carlson (1992) presented *F*-region plasma densities observed on October 7–8, 1991 using the EISCAT IS radar in “Polar” experiment (CP-4) mode. The radar-beam pointed poleward, with an elevation of 20° and an azimuth of 332° from the geographic meridian at Tromsø. The plasma densities measured at this azimuth were more

than  $5 \times 10^5$  el/cm<sup>3</sup>, and showed a characteristic quasi-periodic poleward drift with velocity of about 1 km/s in the invariant latitudes from 71° to 78°. This behavior persisted between about 7 h and 11 h UT, yielding 9 discrete enhancements and hence a mean repetition period of about 25 min (see Fig. 1 of their paper). They identified these features as polar cap “patches” of enhanced plasma densities in the *F*-region ionosphere.

In order to determine whether the daytime absorption features described above are associated with polar cap patches, we use the “Polar” experiment plasma data with an azimuth of 355°, taken between 0700 and 1100 UT on October 8, 1991. At this azimuth, the radar-beam points at the *F*-region ionosphere in the vicinity overhead Ny-Alesund. The plasma data at this azimuth are acquired with a sampling-time of 5 minutes. In Fig. 3, the two beams with azimuths of 332° (labeled 1) and 355° (labeled 2) are shown on a map of the European arctic region. Along the solid line at the azimuth of 355°, measurements at altitudes between 210 km and 648 km in the slant *F*-region ionosphere are marked by dots, whilst the IRIS field (600 km × 600 km) at Ny-Alesund is drawn by a square. On this map, the geomagnetic stations at Svalbard and on the east coast of Greenland are also shown. Below, we shall calculate the absorption value based on the plasma data observed by EISCAT at the azimuth of 355°.

Absorption of radio waves by the ionosphere is usually calculated using the Appleton-Hartree magnetoionic theory. For the riometer used in this study, the radio wave frequency

## OCTOBER 8 1991 NY-ALESUND

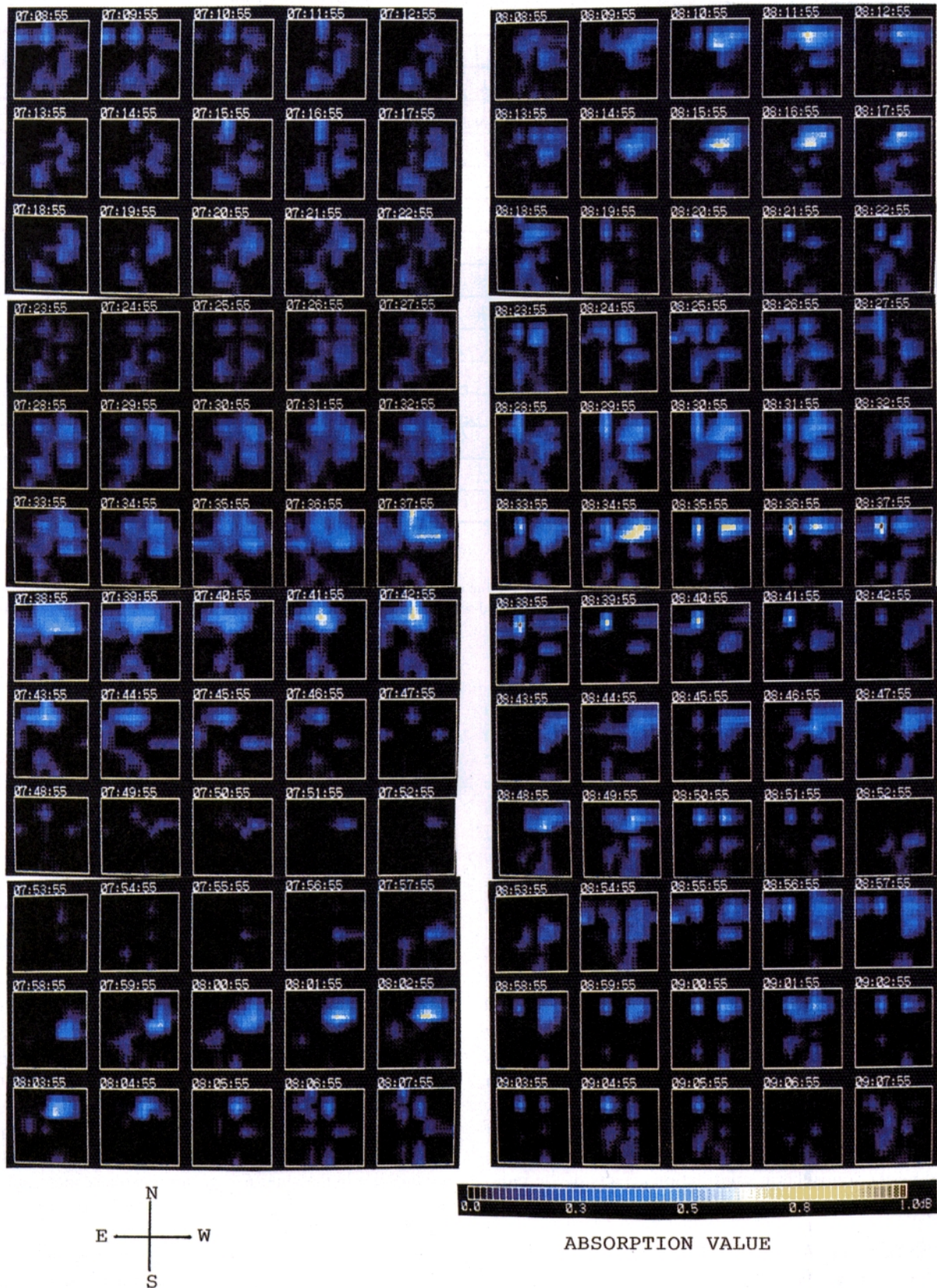


Plate 1. Time series of the absorption images, produced from the 64 IRIS beams, during 0708:56–0907:55 UT on October 8, 1991. Each image is an average over one minute. The absorption scale up to 1 dB is displayed by the color bar.

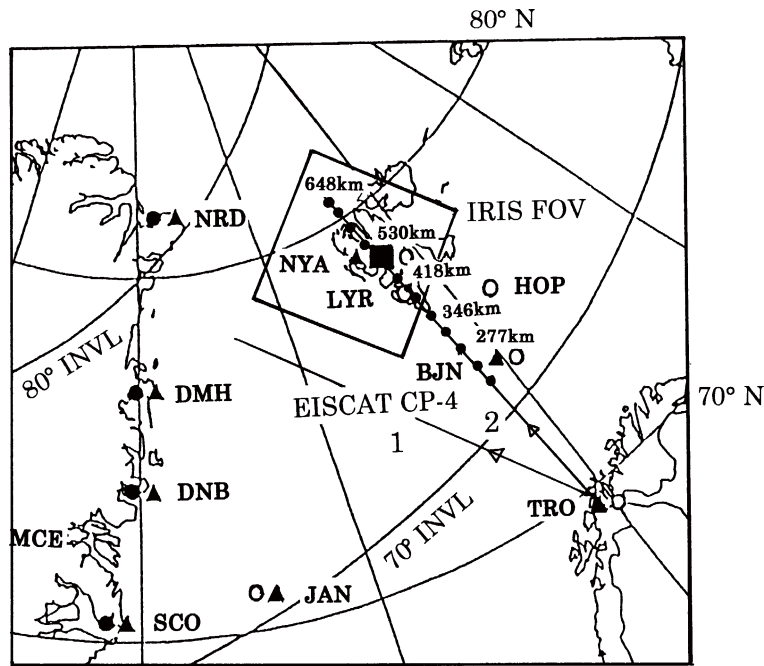


Fig. 3. Beam directions towards azimuths of 332° and 355° made by the EISCAT radar “Polar” experiment (CP-4 mode) on October 8, 1991, drawn on the map of the European arctic region. At the azimuth of 355°, data points of the plasma measurement in the slant range between 210 km and 648 km are shown by dots, and the field of view of the imaging riometer (IRIS) is shown by a square. NYA, HOP, BJA and TRO are the magnetic stations.

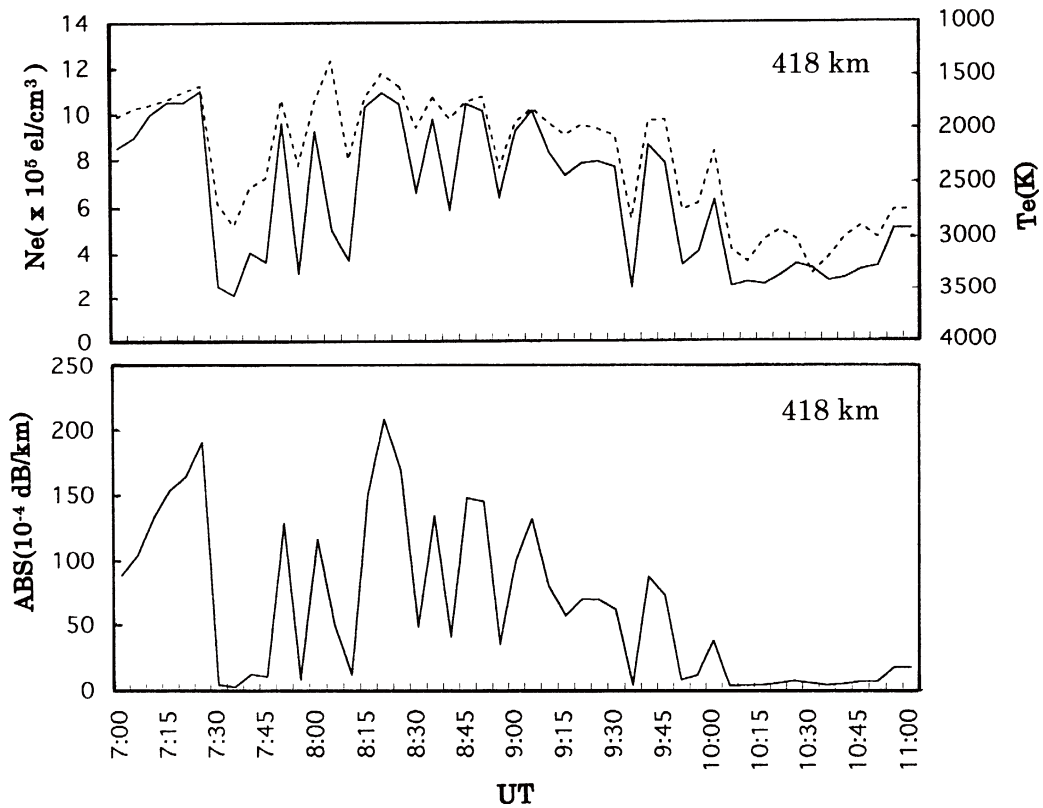


Fig. 4. Upper panel: Time variations of electron densities (solid line) and electron temperatures (broken line) at an altitude of 418 km observed by the EISCAT “Polar” experiment during 0700–1100 UT. Bottom panel: The theoretical absorption value (per km) given by the product of electron densities with effective electron-ion collision frequencies.

(30 MHz) is larger than both the component of the gyro-frequency vector in the direction of propagation, and the collision frequency. Using this approximation, the expression for the absorption  $A$  (dB) is reduced to the following formula (Wang *et al.*, 1994),

$$A = \frac{4.58 \times 10^{-5}}{\omega^2} \int N_e v ds, \quad (1)$$

where  $N_e$  is electron density (in cubic meters),  $v$  the effective electron collision frequency (per second),  $\omega$  the radio wave angular frequency (per second), and  $ds$  the path element (m). In the  $F$ -region ionosphere, the effective electron collision frequency is dominated by electron-ion collisions. Since singly charged  $O^+$  ions dominate the  $F$ -region, for the elastic scattering of electrons by the Coulomb field of ions, we use the following expression for  $v_{e-i}$  (Aggarwal *et al.*, 1979):

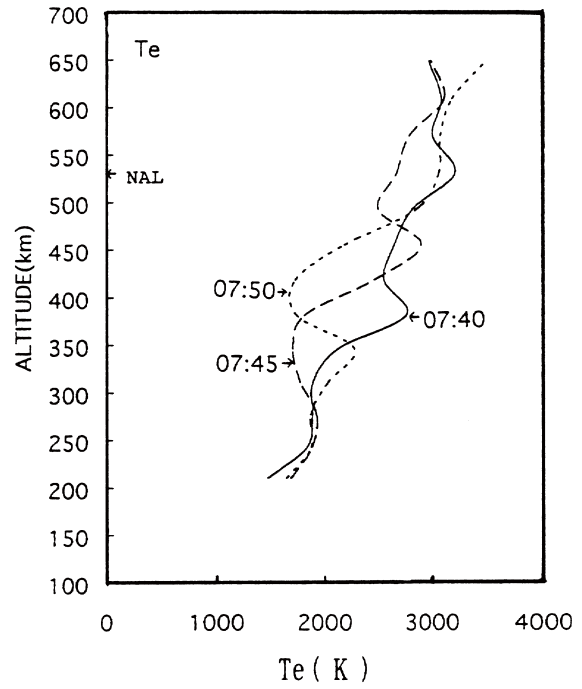
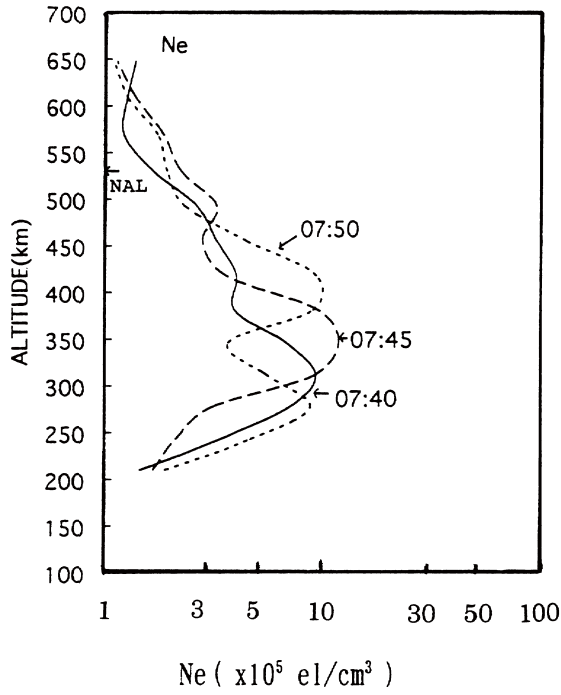


Fig. 5. Altitude profiles of electron densities (left panel) and electron temperatures (right panel) during 0740–0750 UT.

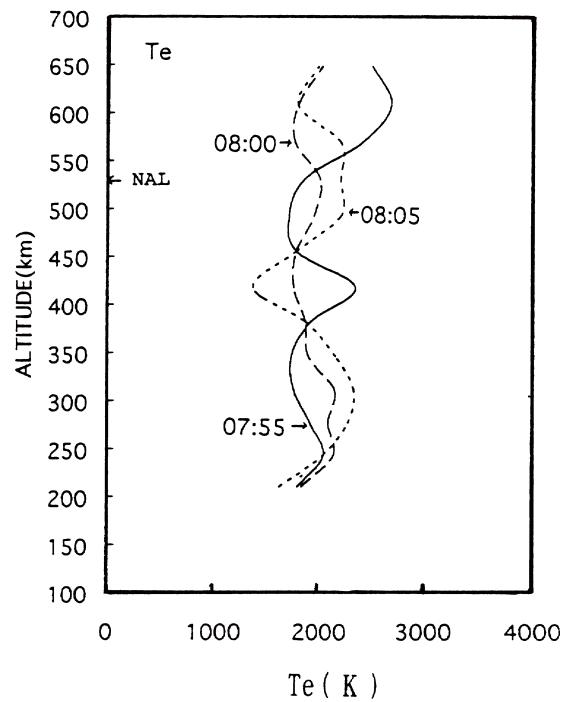
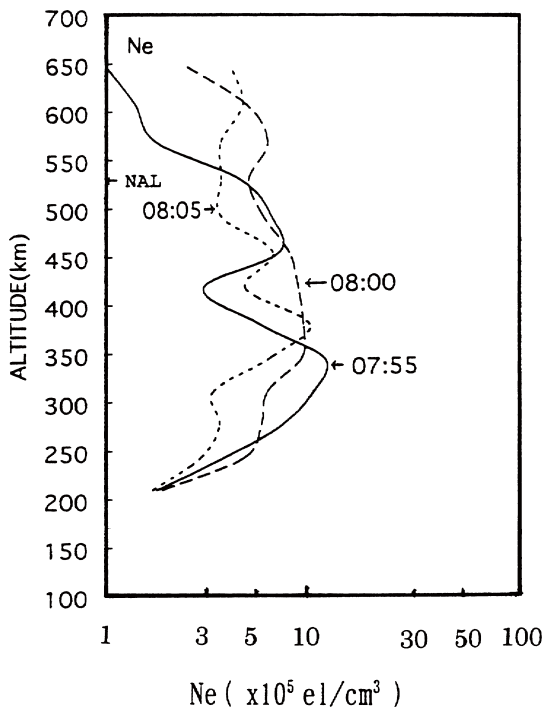


Fig. 6. Altitude profiles of electron densities (left panel) and electron temperatures (right panel) during 0755–0805 UT.

$$v_{e-i} = \left[ 29.4 + 3.64 \ln T_e \left( \frac{2T_e T_i}{N_e (T_e + T_i)} \right)^{1/2} \right] N_e \cdot T_e^{-3/2}. \quad (2)$$

This formula shows that the combination of a high-electron density with a low-electron temperature leads to a high  $v_{e-i}$ , resulting in an increase in the riometer absorption.

The upper panel of Fig. 4 shows the time-variations of electron densities (solid line) and electron temperatures (broken line) at an altitude of 418 km, located within the IRIS field, as shown in Fig. 3. Electron density on the left vertical-line increases upwards, while electron temperature on the right one increases downwards. These variations show a very similar tendency, suggesting that there is no local precipitation of energetic-electrons into the  $F$ -region ionosphere. The lower panel of Fig. 4 shows the time-variation of the product of  $N_e$  and  $v_{e-i}$  calculated from formula (2) at an altitude of 418 km, in units of dB/km. Comparing the product with the absorption values in the N3E7-beam in Fig. 2, the two impulsive peaks at about 0750 UT and 0800 UT coincide well with each other. Some of the other peaks also nearly coincide during 0700–1005 UT. These results indicate that the absorption features near the magnetic noon are associated with electron density enhancements in the  $F$ -region plasma patches.

Here, we further concentrate on two specific time-periods, at 0740–0750 UT (labeled A) and at 0755–0805 UT (labeled B), during which the absorption values are relatively weak (<0.3 dB) and strong (<0.8 dB), respectively. These are shown in the time-varying absorption in the N3E7-beam in Fig. 2. Altitude profiles of electron densities (left panel) and electron temperatures (right panel) are shown in Figs. 5 and 6 for the time-periods (A) and (B), respectively. It should be noted that these profiles are not for vertical altitudes, but for slant ranges in the  $F$ -region ionosphere at the azimuth of  $355^\circ$ , as shown in Fig. 3. During the time-period (A), the electron densities reach peaks of the order of  $10^6$  el/cm<sup>3</sup> at altitudes of 300–400 km. A most pronounced feature is that the peak density shifts higher in the  $F$ -region with time, indicating that the region of enhanced electron densities moved into the IRIS field from a lower-latitude. The velocity of the motion is estimated to be roughly 0.5–1.0 km/s. The temperature peak also shifts higher in the  $F$ -region with time, showing temperatures exceeding 3000 K above 400 km altitude. During the time-period (B) shown in Fig. 6, the density peak shifts higher in the  $F$ -region with time, as is the case for time-period (A). However, the remarkable differences are that the altitude range of the density enhancement is broadened toward the higher  $F$ -region (600 km) at 0800 UT, and that the electron temperatures vary in the vicinity of 2000 K with less of an increase above an altitude of 400 km. Using the altitude profiles in Figs. 5 and 6, the total absorption values integrated through the slant paths from altitudes between 210 km and 648 km are calculated. These are 0.04 dB at 0745 UT during time-period (A), and 0.1 dB at 0800 UT during time-period (B).

#### 4. Discussion

In a dark ionosphere at the South Pole, Rosenberg *et al.*

(1993) recorded daytime absorption values in excess of 1 dB for selected narrow IRIS beams at 38.2 MHz, as described above. They calculated appreciable  $F$ -region absorption (0.3 dB) for the critical frequency,  $f_oF_2$  (the maximum plasma frequency) >9 MHz, by assuming a parabolic electron density layer with a peak at 300 km and a half-width of 200 km, and a temperature profile characteristic of a dark ionosphere (i.e. equal electron and ion temperatures which increase linearly from 200 K to 1000 K between 100 and 300 km, and which remain constant at 1000 K above 300 km). The corresponding  $f_oF_2$  for the ionosonde measurement was about 11.5 MHz. It should be considered, however, that the assumed electron temperatures are smaller than those measured by the EISCAT radar (see Figs. 5 and 6) and by the Sondre Stromfjord IS radar (Wang *et al.*, 1994).

For a sunlit ionosphere, Wang *et al.* (1994) observed  $F$ -region absorption values of 0.3–0.5 dB by IRIS at Sondre Stromfjord, and showed that observed values were larger than that calculated (0.07 dB) using plasma data from a simultaneous IS radar experiment. They indicated that the smaller values are due to a difference, by a factor as high as 4, between the  $v_{e-i}$  calculated by formula (2) above, and the experimentally measured collision frequencies (Setty *et al.*, 1970, Aggarwal *et al.*, 1979).

During 0700–0900 UT on October 8, we observed maximum absorption values of 0.8 dB, as shown in Fig. 2. We derived an absorption value of 0.1 dB using the altitude profiles of the electron densities and collision frequencies between 210 km and 648 km at 0800 UT. However, the calculation was performed for the slant  $F$ -region ionosphere at invariant latitudes from  $71^\circ$  to  $78^\circ$ , as described above. In order to correctly estimate the absorption value for a vertical altitude, we modify the plasma data at 0800 UT, by replacing them with the data at 0750 UT between altitudes of 210 km and 277 km, and the data at 0755 UT between altitudes of 311 km and 381 km. This modification allows for the poleward motion (assuming a velocity of 1 km/s) of the enhanced electron densities and electron temperatures, as shown in Figs. 5 and 6. The modified profiles at 0800 UT are shown in the left (electron densities) and right (electron temperatures) panels of Fig. 7. The modification gives a slightly larger absorption value of 0.14 dB. We notice, however, that this value is still smaller than that observed (0.8 dB), resulting in a difference by a factor of 5–6. This discrepancy may arise if the theoretical electron-ion collision frequency, used in formula (2), is too small compared with the experimentally determined value (see Setty *et al.*, 1970; Aggarwal *et al.*, 1979; and the suggestion by Wang *et al.*, 1994).

Another complicating factor is that absorption by the lower  $E$ - or  $D$ -region ionosphere may have contributed to the total absorption observed. The “Polar” experiment of EISCAT cannot obtain plasma data below an altitude of 210 km. An ionosonde, which is a powerful tool for evaluating electron density enhancement in the lower ionosphere, was not installed in September, 1991. Here we show the geomagnetic  $H$ -component data obtained at Ny-Alesund (NYA), Hopen (HOP), Bjornoya (BJN) and Tromso (TRO), which are aligned near an azimuth of  $355^\circ$  (see the map in Fig. 3). Figure 8 shows the time variations of the  $H$ -component during

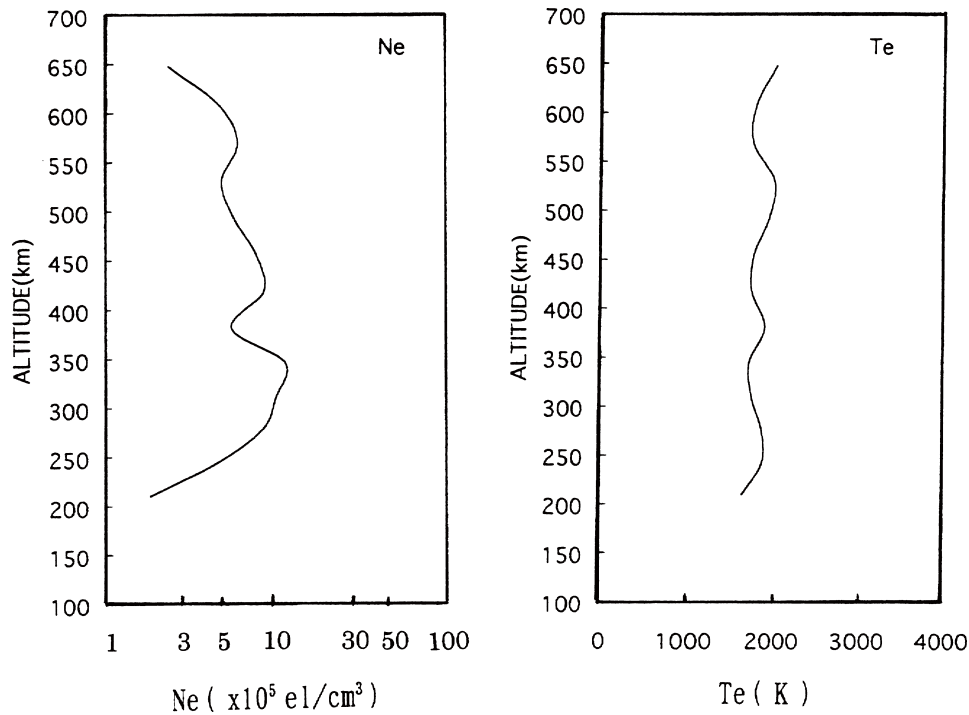


Fig. 7. Modified altitude profiles of electron densities (left panel) and electron temperatures (right panel) at 0800 UT.

0600–1100 UT on October 8, 1991. From the rather smooth variation of the  $H$ -component during 0700–1000 UT at Ny-Alesund, we can predict that the absorption by the lower  $E$ - or  $D$ -region due to the precipitation of high energy particles is very weak.

The DMSP F9 satellite passed between the morning sector (0900–1000 MLT) at the latitude of Ny-Alesund and the central polar cap during about 0755–0800 UT and 0935–0940 UT on two successive passes on October 8. The energy/time spectrogram of the precipitating electrons from 32 eV to 30 keV energy range shows the polar cap boundary ( $\sim 72^\circ$  MLAT) between BPS (“Boundary Plasma Sheet”) and CPS (“Central Plasma Sheet”) in the morning sector (Newell and Meng, 1992), and also very low integral energy flux of  $10^7\text{--}8 \text{ keV}/(\text{cm}^2\text{s sr})$  for the soft electrons (polar rain of  $<300 \text{ eV}$ ) at the latitude of Ny-Alesund (not shown). However, since the satellite didn’t pass inside the IRIS field of view over Ny-Alesund, we cannot exactly predict the precipitation of high energy electrons into the lower ionosphere.

In order to estimate the absorption value in the lower  $E$ - and  $D$ -region, we use the undisturbed electron density profiles in the altitude range between 80 and 160 km derived from the EISCAT measurements (Kirkwood, 1993). These profiles are labeled by the corresponding solar-zenith angle, at both low and high solar activity levels. In 1991, solar activity was high, and on October 8 at Ny-Alesund the solar-zenith angle near the magnetic noon was between  $85^\circ$  and  $90^\circ$  during the present absorption event. The integrated absorption value between altitudes of 80 and 160 km, calculated from the electron densities and the effective electron-neutral collision frequencies given by Aggarwal *et al.* (1979), becomes about 0.09 dB. This absorption value is generally below the minimum detectable level (0.1 dB) of the narrow-beam

riometer. Thus from these discussions, we can indicate that absorption in the lower  $E$ - or  $D$ -region caused by the precipitation of energetic particles has a negligible contribution to the observed absorption.

We show in Plate 1 that around 0740 UT, the initially widespread absorption in the IRIS field is localized and enhanced in the northern sector ( $76^\circ\text{--}78^\circ$  INV L), and follows a poleward motion. Thereafter, a similar behavior appears quasi-periodically, with an eastward component in the motion. Simultaneous EISCAT observations showed that the patches of  $F$ -region plasma with enhanced electron density drifted poleward (anti-sunward) from the polar cusp into the cap ( $78^\circ$  INV L), with a mean repetition of 25 min near the magnetic noon (Lockwood and Carlson, 1992). This coincidence suggests that the observed daytime absorption features are associated with the  $F$ -region plasma patches drifting poleward. However, we notice a difference, in that the enhanced absorption features are localized only in the higher-latitude sector of the IRIS field, whilst the plasma patches detected by the IS radar extend from the polar cusp to the cap ( $71^\circ\text{--}78^\circ$  INV L). Such a difference was also seen between the ionospheric absorption features observed at the South Pole, and the echo patterns observed by the PACE HF radar (Rosenberg *et al.*, 1993). Below, we briefly discuss this problem in relation to the formation and propagation of plasma patches.

Anderson *et al.* (1988) proposed a mechanism for the formation of polar plasma patches. In this model, the cross polar-cap potential rises abruptly, causing an increase in the size of the convection pattern. This in turn brings the sunlit high-concentration  $F$ -region plasma from low geomagnetic latitudes into the vicinity of the polar cusp, thereafter the plasma propagates into the polar cap. Using the Millstone Hill IS radar data, Foster (1993) revealed that enhancements



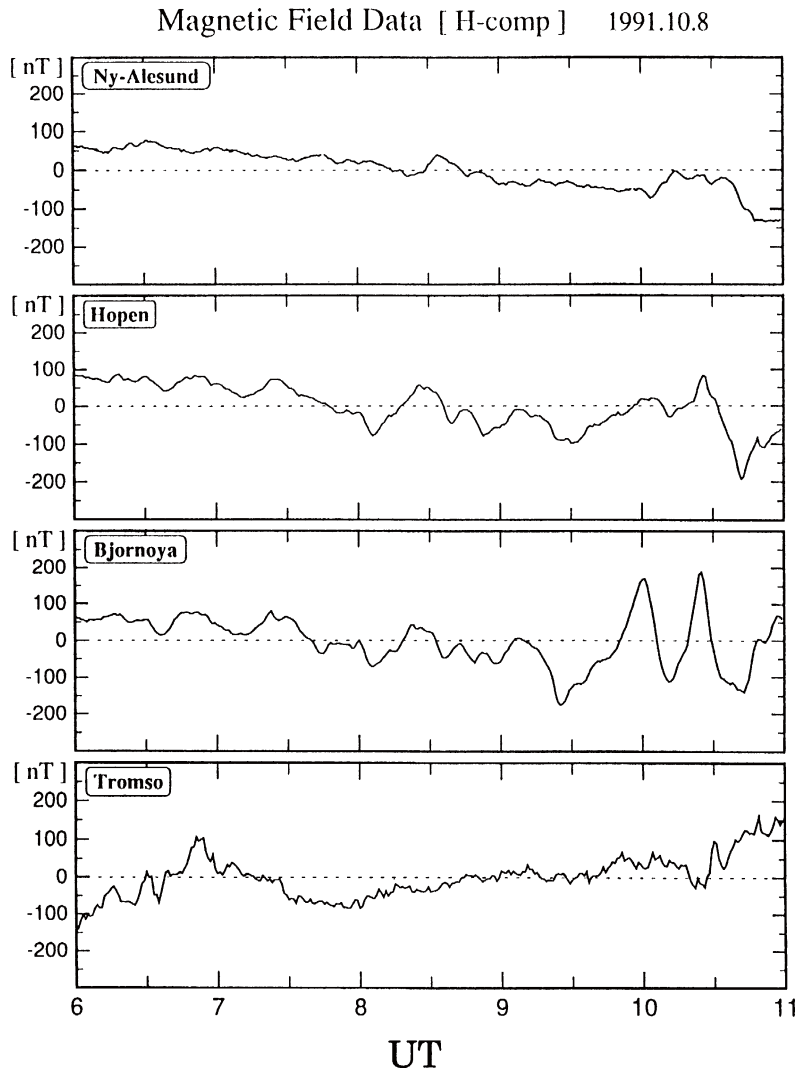


Fig. 8. Time variations of the geomagnetic  $H$ -component during 0600–1100 UT on October 8, 1991 at Ny-Alesund, Hopen, Bjornoya and Tromso.

of solar-produced plasma occurred in the afternoon sector near the equatorward edge of the convection pattern. This plasma then convected towards noon through the polar cusp, and propagated into the polar cap. These proposed mechanisms rely on the presence of large gradients in the electron concentration close to the equatorward edge of the convection pattern in the solar-produced plasma. On the contrary, polar plasma patches are observed when the solar terminator is not close to the equatorward edge of the convection pattern (Baker *et al.*, 1989; Lockwood and Carlson, 1992).

Using PACE HF radar data, Rodger *et al.* (1994) recently proposed a new mechanism, in which the precipitation of energetic particles into the cusp and boundary layer can play a more important role in the formation of enhanced plasma convection near the magnetic noon. The patch itself forms through the disruption of ionospheric convection caused by the simultaneous effects imposed by the presence of a flow channel event, FCE (short-lived plasma jets), and the re-organization of the flow pattern caused by changes in the  $B_y$ -component of the IMF. After formation, the patches move poleward in bulk, with the same velocity as the plasma within the patch, under the influence of  $\mathbf{E} \times \mathbf{B}$  force. During October 7–8, IMP 8 was located on the dusk-side in the solar

wind. Unfortunately, IMF data from IMP 8 are missing during the period of about 0130–1500 UT, including the period of the absorption event, thus we are unable to discuss the effect of IMF change on patch formation.

In stead of IMF data, in Fig. 9, we show a pattern of equivalent ionospheric convection vectors at 0800 UT during the time-period (B). The vectors are derived from the magnetometer networks along the east and west coasts of Greenland, and they are drawn in an invariant latitude (INVL)-eccentric dipole time (EDT) coordinate system. The plots include the vertical magnetic component, which gives information on the position of the current system. The equatorward prevailing convection vectors change gradually from sunward at 0730 EDT to anti-sunward near 0930 EDT, but show no pronounced change in a series of convection vector patterns produced every 10 min during the absorption event. This may indicate that the re-organization of flow pattern caused by an IMF  $B_y$  change is less likely.

Lockwood and Carlson (1992) considered that transient bursts of magnetic reconnection, or “flux transfer events” FTEs (termed by Russel and Elphic (1978)), at the dayside magnetopause may be a cause of the polar cap “patches”. Using the model adapted from Cowley *et al.* (1991), they

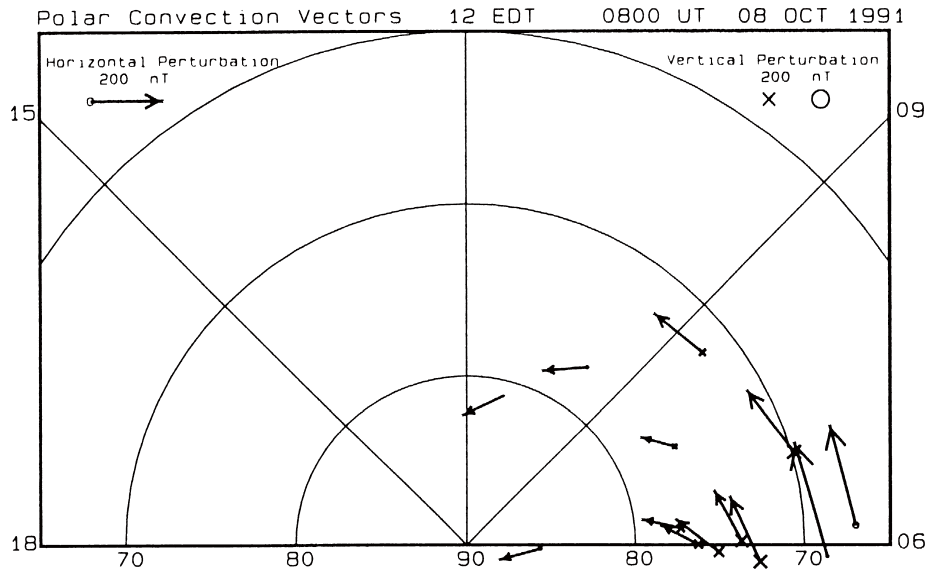


Fig. 9. Equivalent ionospheric convection vectors at 0800 UT, derived from the geomagnetic data collected at the chain stations along the east and west coasts of Greenland on October 8, 1991. The vectors are drawn in the invariant latitude (INVL)-eccentric dipole time (EDT) coordinate system.

illustrated that a sequence of reconnection pulses, at about 20 minute intervals, caused the merging gap to migrate towards the equator. This mechanism was based upon the observations of poleward moving patches by EISCAT IS radar, which were simultaneous with the present absorption event. From the IS radar and satellite particle observations, Lockwood *et al.* (1993) revealed that the particles precipitating into the polar cusp ionosphere had the characteristics of originating from the shocked solar-wind plasma of the magnetosheath, and that the series of discrete, poleward moving plasma structures were consistent with the “pulsating cusp model” (Lockwood and Smith, 1992).

Of the  $H$ -component variations at the four magnetic stations shown in Fig. 8, the  $H$ -component at Ny-Alesund ( $76.1^\circ$  INVL) shows a rather smooth variation during 0700–1000 UT, whilst the one at Bjornoya ( $71.4^\circ$  INVL) shows small negative-bays ( $\sim 50$  nT) with short duration ( $\sim 10$  min) at about 0740 UT, 0800 UT, 0815 UT, 0835 UT, 0845 UT and 0855 UT, and slightly larger ones ( $\sim 150$  nT) at 0925 UT and 1015 UT. Evidently, these bays correspond to the respective absorption peaks shown in Fig. 2. An evident correspondence is also seen between the small magnetic bays at Hopen ( $72.9^\circ$  INVL) and the absorption peaks. During the absorption event, the both stations at Bjornoya and Hopen would be located near the polar cusp. On the other hand, no corresponding bay is seen at Tromso ( $66.7^\circ$  INVL), located equatorward of the dayside auroral oval. Sandholt *et al.* (1986) revealed that, at meridian magnetic stations, magnetic  $H$ -deflections from the polar cusp to the cap are associated with the poleward moving transient luminosity of the cusp aurora in the post-noon sector, and that this cusp aurora is likely a signature of plasma transfer from the magnetosheath. Thus, the good correspondence between the  $H$ -deflections and the absorption peaks indicates that the precipitation of magnetosheath-like particles into the cusp ionosphere contributes to the formation of plasma patches, and that the products move towards the polar cap. From EISCAT plasma flow observations, Lockwood *et al.* (1990) demonstrated that,

from magnetic noon to post noon, the plasma flows at Ny-Alesund latitude increased in speed (2–4 km/s), and the flow direction rotated from northward to eastward. This rotation in the plasma flow direction may cause small-scale irregularities, due to density gradients in the enhanced northward moving flows. Consequently, these small-scale irregularities may cause the localized and enhanced absorption features showing northward motion with eastward component in the high-latitude section of the IRIS field.

## 5. Conclusion

Based on the observations and discussions, we conclude that the ionospheric absorption features observed near the magnetic noon at Ny-Alesund are associated with plasma patches with enhanced electron density in the  $F$ -region ionosphere, which are drifting poleward from the cusp to the cap. The observed absorption values are larger than the theoretical value, estimated from the electron densities and electron-ion collision frequencies derived from the data of a simultaneous “Polar” EISCAT observation of the  $F$ -region ionosphere. This discrepancy seems to be due to the difference between the calculated collision frequencies and the experimental ones, as indicated by Wang *et al.* (1994). The localized and enhanced absorption features, which show poleward motion in the high-latitude section of the IRIS field at Ny-Alesund, may be explained by the following processes. Magnetosheath-like particles precipitate into the polar cusp due to transient bursts of magnetic reconnection in the dayside magnetopause. This results in the formation of plasma patches at the cusp-latitude, which drift poleward into the polar cap  $F$ -region ionosphere. The drifting patches cause small-scale irregularities above Ny-Alesund through density gradients in the plasma flows. The imaging riometer could observe the localized, enhanced absorption features caused by small-scale irregularities. Further simultaneous observations with the same coverage should be performed by an imaging riometer, an IS radar and an HF radar, to obtain a more definite relationship between the  $F$ -region

ionospheric absorption features and the poleward drifting plasma patches.

**Acknowledgments.** We are grateful to the help offered by the Director and staff at EISCAT. EISCAT is supported by the Research Councils of France (CNRS), Germany (MPG), Norway (NAVY), Sweden (NFR), Finland (SA), UK (SERG) and Japan (NIPR). We would also like to thank A. Egeland, University of Oslo, for arranging the riometer observations at Ny-Alesund; and T. Ogawa, Nagoya University, for helpful comments. We acknowledge P. T. Newell and C. I. Meng, Johns Hopkins University, for the provision of DMSP-F9 particle spectrograms; T. Hansen, University of Tromso, for the provision of magnetic data; and P. Stauning, Danish Meteorology Institute, for fruitful discussion and provision of plasma convection vectors derived from the Greenland geomagnetic data.

## References

- Aggarwal, K. M., Narinder Nath, and C. S. K. Setty, Collision frequency and transport properties of electrons in the ionosphere, *Planet. Space Sci.*, **27**, 753–768, 1979.
- Anderson, D. N., J. Buchau, and R. A. Heelis, Origin of density enhancements in the winter polar cap ionosphere, *Radio Sci.*, **23**, 513–519, 1988.
- Baker, K. B., R. A. Greenwald, J. M. Ruohoniemi, J. R. Dedeny, M. Pinnock, N. Mattin, and J. M. Leonard, PACE, Polar Anglo-American Conjugate Experiment, *EOS Trans. AGU*, **70**, 785, 1989.
- Cowley, S. W. H., M. P. Freeman, M. Lockwood, and M. F. Smith, The ionospheric signature of flux transfer events, in *CLUSTER-Dayside Polar Cusp*, ESA SP-330, pp. 105–112, ESTEC, Noordwijk, The Netherlands, 1991.
- Detrick, D. L. and T. J. Rosenberg, A phased-array radio wave imager for studies of cosmic noise absorption, *Radio Sci.*, **25**, 325–338, 1990.
- Foster, J. C., Storm time plasma transport at middle and high latitude, *J. Geophys. Res.*, **98**, 1675–1689, 1993.
- Kirkwood, S., Modeling the undisturbed high-latitude region, *Adv. Space Res.*, **13**, 3, 101–104, 1993.
- Lockwood, M. and H. C. Carlson, Jr., Production of polar cap electron density patches by transient magnetopause reconnection, *Geophys. Res. Lett.*, **19**, 1731–1734, 1992.
- Lockwood, M. and M. F. Smith, The variation of reconnection rate at the dayside magnetopause and cusp ion precipitation, *J. Geophys. Res.*, **97**, 14,841–14,847, 1992.
- Lockwood, M., P. E. Sandholt, A. D. Farmer, S. W. H. Cowley, B. Lybakk, and V. N. Davda, Auroral and plasma flow transients at magnetic noon, *Planet. Space Sci.*, **38**, 8, 973–993, 1990.
- Lockwood, M., W. F. Denig, A. D. Farmer, V. N. Davda, S. W. H. Cowley, and H. Luhr, Ionospheric signatures of pulsed reconnection at the Earth's magnetopause, *Nature*, **361**, 4, 424–428, 1993.
- Newell, P. T. and C. I. Meng, Mapping the dayside ionosphere to the magnetosphere according to particle precipitation characteristics, *Geophys. Res. Lett.*, **19**, 6, 609–612, 1992.
- Nishino, M., Y. Tanaka, T. Oguti, H. Yamagishi, and J. A. Holtet, Initial observation results with imaging riometer at Ny-Alesund ( $L = 16$ ), *Proc. NIPR Symposium on Upper Atmosphere Physics*, No. 6, 47–61, 1993.
- Nishino, M., H. Yamagishi, P. Stauning, T. J. Rosenberg, and J. A. Holtet, Location, spatial scale and motion of radio wave absorption in the cusp-latitude ionosphere observed by imaging riometers, *J. Atmos. Terr. Phys.*, **59**, 8, 903–924, 1997.
- Rodger, A. S., M. Pinnock, J. R. Dudeney, K. B. Baker, and R. A. Greenwald, A new mechanism for polar patch formation, *J. Geophys. Res.*, **99**, 6425–6436, 1994.
- Rosenberg, T. J., Z. Wang, A. S. Rodger, J. R. Dudeney, and K. B. Baker, Imaging riometer and HF radar measurements of drifting  $F$  region electron density structures in the polar cap, *J. Geophys. Res.*, **98**, 7757–7764, 1993.
- Russell, C. T. and R. C. Elphic, Initial ISEE magnetometer results: Magnetopause observations, *Space Sci. Rev.*, **22**, 681–715, 1978.
- Sandholt, P. E., C. S. Dehr, A. Egeland, B. Lybakk, R. Viereck, and G. L. Romick, Signatures in the dayside aurora of plasma transfer from the magnetosheath, *J. Geophys. Res.*, **91**, A9, 10,063–10,079, 1986.
- Setty, C. S. G. K., A. R. Jain, and M. K. Vyawahare, Collision frequency of electrons in the  $F$ -region, *Can. J. Phys.*, **48**, 653–658, 1970.
- Stauning, P., Absorption of cosmic noise in the  $E$ -region during electron heating events. A new class of riometer absorption events, *Geophys. Res. Lett.*, **11**, 1184–1187, 1984.
- Stauning, P., Investigations of ionospheric radio wave absorption processes using imaging riometer techniques, *J. Atmos. Terr. Phys.*, **58**, 6, 753–764, 1996a.
- Stauning, P., High-latitude  $D$ - and  $E$ -region investigations using imaging riometer observations, *J. Atmos. Terr. Phys.*, **58**, 6, 765–783, 1996b.
- Stauning, P. and J. K. Olesen, Observations of the unstable plasma in the disturbed polar  $E$ -region, *Physica Scripta*, **40**, 325–332, 1989.
- Wang, Z., T. J. Rosenberg, P. Stauning, S. Basu, and G. Crowley, Calculations of riometer absorption associated with  $F$  region plasma structures based on Sondre Stromfjord incoherent scatter radar observations, *Radio Sci.*, **29**, 209–215, 1994.
- Yamagishi, H., M. Nishino, M. Sato, Y. Kato, M. Kojima, N. Sato, and T. Kikuchi, Development of imaging riometers, *Antarctic Record*, **36**, 2, 227–250, 1992 (in Japanese).

---

Masanori Nishino (e-mail: nishino@stelab.nagoya-u.ac.jp), Satonori Nozawa (e-mail: nozawa@stelab.nagoya-u.ac.jp), and Jan A. Holtet (e-mail: j.a.holtet@fys.uio.no)